

Synthesis and characterization of $\text{Ni}_{0.6}\text{Zn}_{0.4}\text{Fe}_2\text{O}_4$ nano-particles obtained by auto catalytic thermal decomposition of carboxylato-hydrazinate complex

U. B. Gawas · V. M. S. Verenkar · S. C. Mojumdar

CTAS2010 Conference Special Chapter
© Akadémiai Kiadó, Budapest, Hungary 2011

Abstract $\text{Ni}_{0.6}\text{Zn}_{0.4}\text{Fe}_2\text{O}_4$ nano-particles have been synthesized by self-propagating auto-combustion of nickel zinc ferrous fumarato-hydrazinate complex. The precursor complex has been characterized by chemical analysis, IR, AAS, thermal analysis and isothermal mass loss studies. The precursor on ignition undergoes self-propagating auto combustion to give $\text{Ni}_{0.6}\text{Zn}_{0.4}\text{Fe}_2\text{O}_4$. The X-ray diffraction studies confirmed the single phase formation of nano-size ‘as synthesized’ $\text{Ni}_{0.6}\text{Zn}_{0.4}\text{Fe}_2\text{O}_4$. TEM observation showed the average particle size to be 20 nm. Infrared and magnetization studies were also carried out on the ‘as synthesized’ $\text{Ni}_{0.6}\text{Zn}_{0.4}\text{Fe}_2\text{O}_4$. The lower value of saturation magnetization and higher Curie temperature of ‘as synthesized’ ferrite also hint at the nano size nature.

Keywords Nano-particles · TG · DSC · FTIR · XRD · TEM

Introduction

Nanocrystalline ferrites are the materials of current interest because of their unique electric, dielectric, magnetic and

optical properties which make them appealing from theoretical and technological point of view [1]. Ni-Zn ferrites are soft ferrimagnetic materials with low magnetic coercivity and high resistivity [2]. The eddy current losses are also low for these materials in high frequency operations [3]. Because of these properties, Ni-Zn ferrites find application in core material for power transformer in electronics recording media heads, antenna rods, loadies coil, microwave devices and telecommunication applications [4]. Recently, the nanocrystalline magnetic materials are used in biomedicine and biotechnology as contrast agent in magnetic resonance imaging (MRI) and also as drug carriers for magnetically guide drug delivery [5]. The structure as well as magnetic properties of the ferrites is found to depend upon the method of synthesis [6]. Wet chemical methods offer better properties like small particle size, low temperature of formation, stoichiometrically pure materials over the wide range of temperature [7]. Various wet chemical methods like co-precipitation [8], citrate precursor [9], sol-gel [10], combustion [11–13], flash combustion [14] and carboxylate precursor method [15] have been reported for the synthesis of Ni-Zn ferrites. There has been considerable interest among researchers in the study of hydrazine derivatives of metal carboxylates since they serve as precursors to fine particle oxide materials relatively at much lower temperatures.

Recently, many such combustion synthesis of metal and mixed metal oxides using metal carboxylate and carboxylato-hydrazinates complexes of oxalate [16], formate [17, 18], acetate [18, 19] and propionate [19], malonate, succinate and itaconates [20–24], maleate and tartrate [25, 26] malate [27] and fumarate [28–34] have been studied. In the present investigation, synthesis of nano-size nickel zinc ferrite using novel fumarato-hydrazinate complex as precursor has been reported.

U. B. Gawas · V. M. S. Verenkar
Department of Chemistry, Goa University, Taleigao Plateau,
Goa 403206, India

S. C. Mojumdar (✉)
Department of Chemical Technologies and Environment,
Faculty of Industrial Technologies, Trenčín University
of A. Dubcek, Puchov, Slovakia
e-mail: scmojumdar@yahoo.com

S. C. Mojumdar
University of New Brunswick, Saint John, NB E2L 4L5, Canada

Experimental

Preparation of nickel zinc ferrous fumarato-hydrazinate complex

A requisite quantity of sodium fumarate in aqueous medium was stirred with hydrazine hydrate (99–100%) in an inert atmosphere for 2 h. To this solution, a stoichiometric amount of freshly prepared ferrous chloride solution mixed with nickel chloride and zinc chloride was added dropwise with constant stirring in an inert atmosphere. The yellow-coloured precipitate thus obtained was filtered off, washed with ethanol, dried with diethyl ether and then stored in vacuum desiccators.

Characterization

The hydrazine content in the precursor was determined by volumetric analysis using standard 0.025 M KIO_3 solution under Andrew's conditions [35]. The metal contents were determined using atomic absorption spectrophotometer model 201 Chemita. The structure and phase purity of the nickel manganese zinc ferrite (as prepared) was determined by Philips X-ray diffractometer model PW 1710 with Cu K_α radiations and Ni filter. Simultaneous thermogravimetric and differential scanning calorimetry of 'as synthesized' nickel zinc ferrite was recorded on a NETZSCH DSC-TG STA 409PC at a heating rate of 10 °C per min. The isothermal and total mass loss studies of the precursor were carried out along with hydrazine estimation at various predetermined temperatures. Infrared analysis of the precursor and the ferrite was done on FTIR Shimadzu IR prestige21 series spectrophotometer. Transmission electron micrograph (TEM) and energy-dispersive X-ray analysis (EDX) were carried out on Philip's-CM20 electron microscope. The saturation magnetization of the ferrite was measured on alternating current hysteresis loop tracer described Likhite et al. [36] and supplied by M/s Prutha Electronics, Mumbai, India. Curie temperature was determined from the variation of AC susceptibility as a function of temperature as described by Likhite et al. [37].

Autocatalytic decomposition of the complex

For autocatalytic decomposition, the precursor was uniformly spread over a Petri dish, and a burning splinter was

brought near to it, when small portion of it caught fire. A red glow that formed spread over the entire bulk completing the total decomposition of the precursor in an ordinary atmosphere at a temperature as low as 340 °C. This 'as synthesized' nickel zinc ferrite powder was then pelletized under a pressure of 7 tones per square inch for 3 min.

Result and discussion

Chemical formula fixation of nickel zinc ferrous fumarato-hydrazinate complex

A chemical formula of $\text{Ni}_{0.6}\text{Zn}_{0.4}\text{Fe}_2(\text{C}_4\text{H}_2\text{O}_4)_3\cdot6\text{N}_2\text{H}_4$ for precursor complex has been fixed based on the total percentage mass loss and percentage of hydrazine, nickel, zinc and iron which match closely with the calculated values (Table 1). The precursor is found to loose hydrazine ~170 °C when heated isothermally. The infrared spectra of the precursor (Fig. 1) show three bands in the region 3190–3352 cm^{-1} due to the N–H stretching frequencies and in the range of 1552–1583 cm^{-1} due to NH_2 deformation. The N–N stretching frequency is observed at 972 cm^{-1} which confirms the bidentate bridging nature of hydrazine ligand [38, 39]. The asymmetric and symmetric stretching frequencies of the carboxylic ion in the precursor are seen at 1628 and 1384 cm^{-1} , respectively with $\Delta\nu(\nu_{\text{asy}} - \nu_{\text{sym}})$ separation of 244 cm^{-1} indicating the monodentate linkage of both carboxylate groups in the dianions [40]. Thus, the fumarate dianions in the complex coordinate to the metal as bidentate ligand via both the carboxylate groups. These results suggest the formation of nickel zinc ferrous fumarato-hydrazinate complex. Infrared spectrum of the 'as synthesized' $\text{Ni}_{0.6}\text{Zn}_{0.4}\text{Fe}_2\text{O}_4$ shows high frequency ν_1 and low frequency ν_2 bands at 595 and 425 cm^{-1} , respectively, which match closely with the reported values [41].

Thermal analysis and phase identification of product

The TG curve (Fig. 2) of $\text{Ni}_{0.6}\text{Zn}_{0.4}\text{Fe}_2(\text{C}_4\text{H}_2\text{O}_4)_3\cdot6\text{N}_2\text{H}_4$ in air from room temperature to 800 °C shows four mass loss regions with two major ones. The mass loss of 4.86 and 26.98% from room temperature to 110 °C and from 110 to 150 °C (Table 2) were due to the loss of one hydrazine and

Table 1 Chemical analysis and total mass loss studies of nickel zinc ferrous fumarato-hydrazinate complex, $\text{Ni}_{0.6}\text{Zn}_{0.4}\text{Fe}_2(\text{C}_4\text{H}_2\text{O}_4)_3\cdot6\text{N}_2\text{H}_4$

Complex	Nickel/%		Zinc/%		Iron/%		Hydrazine/%		Total mass loss/%	
	Obs.	Calc.	Obs.	Calc.	Obs.	Calc.	Obs.	Calc.	Obs.	Calc.
$\text{Ni}_{0.6}\text{Zn}_{0.4}\text{Fe}_2(\text{C}_4\text{H}_2\text{O}_4)_3\cdot6\text{N}_2\text{H}_4$	4.68	4.98	3.43	3.70	15.81	15.79	27.24	27.18	66.86	66.49

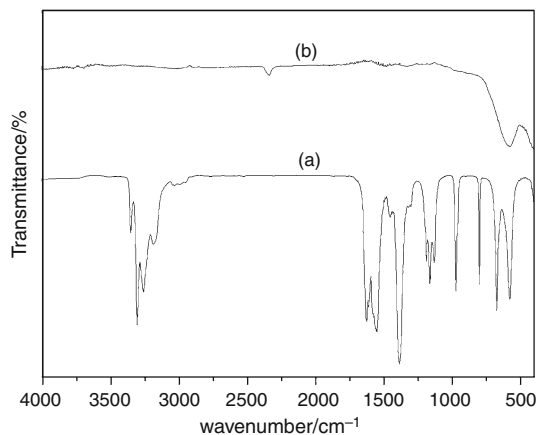


Fig. 1 FT-IR spectra of (a) $\text{Ni}_{0.6}\text{Zn}_{0.4}\text{Fe}_2(\text{C}_4\text{H}_2\text{O}_4)_3 \cdot 6\text{N}_2\text{H}_4$ precursor and (b) ‘as synthesized’ $\text{Ni}_{0.6}\text{Zn}_{0.4}\text{Fe}_2\text{O}_4$

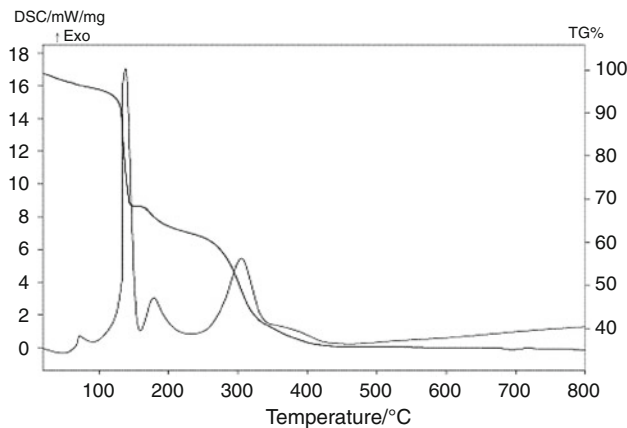


Fig. 2 TG-DSC curves of $\text{Ni}_{0.6}\text{Zn}_{0.4}\text{Fe}_2(\text{C}_4\text{H}_2\text{O}_4)_3 \cdot 6\text{N}_2\text{H}_4$

five hydrazine molecules, respectively. DSC shows two sharp exotherms with a peak temperature of 130 and 144 °C due to two-step dehydrazination. The major mass loss of 39.26% on TG curve from 150 to 350 °C can be attributed to the decarboxylation of the dehydrazinated precursor. DSC curve shows two exothermic peaks in this

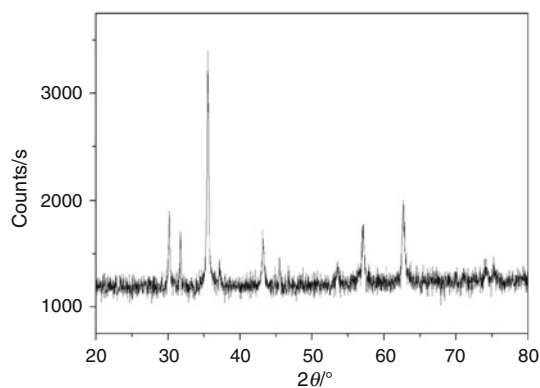


Fig. 3 XRD pattern of ‘as synthesized’ $\text{Ni}_{0.6}\text{Zn}_{0.4}\text{Fe}_2\text{O}_4$

region with the peak temperature of 180 and 306 °C due to two-step oxidative decarboxylation. A marginal mass loss of 3.8% in the region 350–440 °C may be due to unburned carbon which is indicated on the DSC curve by a broad exothermic peak in this region.

The complex decomposes autocatalytically at room temperature once ignited to give nano-size nickel zinc ferrite (as synthesized). The X-ray diffraction pattern of ‘as synthesized’ nickel zinc ferrite (Fig. 3) not only confirms the single phase formation of the ferrite but also the nano-size nature. The X-ray diffraction data such as d-values and lattice parameter of ‘as synthesized’ $\text{Ni}_{0.6}\text{Zn}_{0.4}\text{Fe}_2\text{O}_4$ matches closely with the reported values [42].

The TEM image (Fig. 4) of ‘as synthesized’ $\text{Ni}_{0.6}\text{Zn}_{0.4}\text{Fe}_2\text{O}_4$ shows the average particle size of 20 nm. The saturation magnetization of ‘as synthesized’ $\text{Ni}_{0.6}\text{Zn}_{0.4}\text{Fe}_2\text{O}_4$ was found to be 49.6 emu/g, which is lower than the reported value for bulk $\text{Ni}_{0.6}\text{Zn}_{0.4}\text{Fe}_2\text{O}_4$ [43]. The reason for the lower value of saturation magnetization is the high porosity and the small particle size of ‘as synthesized’ nickel zinc ferrite. It has been reported that particles with higher surface area and very small size have lower magnetization values [44]. The plot of AC susceptibility against temperature of nickel zinc ferrite indicates that the sample

Table 2 TG-DSC, isothermal mass loss and chemical analysis data of nickel zinc ferrous fumarato-hydrazinate complex, $\text{Ni}_{0.6}\text{Zn}_{0.4}\text{Fe}_2(\text{C}_4\text{H}_2\text{O}_4)_3 \cdot 6\text{N}_2\text{H}_4$

TG	Temp. range/°C	DSC	Remarks	Isothermal mass loss/chemical analysis		
				Temp. range/°C	Mass loss/%	$\text{N}_2\text{H}_4/\%$
RT–110	4.86	73.2 (exo)	Loss of one N_2H_4 molecule	RT–100	4.69	23.87
110–150	26.98	144 (exo)	Loss of five N_2H_4 molecule	100–125	55.44	Compd. catches fire
150–226	5.87	180 (exo)	Multistep decarboxylation			
226–353	22.57	306 (exo)				
353–438	3.82	360–390 (broad exo hump)				

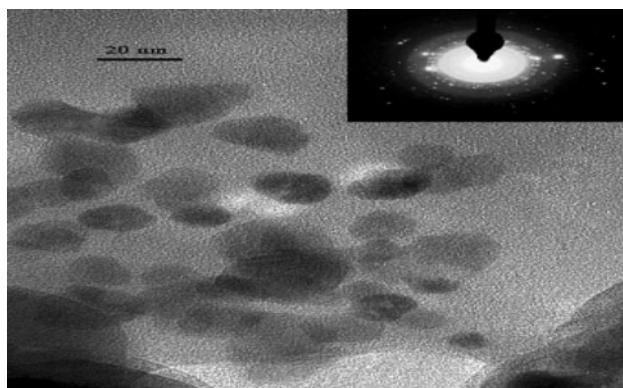


Fig. 4 TEM image of ‘as synthesized’ $\text{Ni}_{0.6}\text{Zn}_{0.4}\text{Fe}_2\text{O}_4$

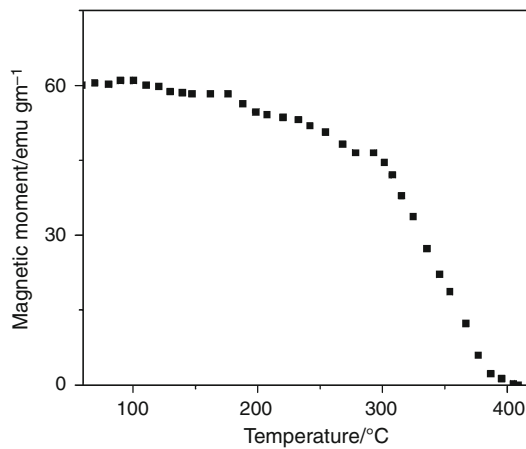


Fig. 5 Plot of AC susceptibility versus temperature for ‘as synthesized’ $\text{Ni}_{0.6}\text{Zn}_{0.4}\text{Fe}_2\text{O}_4$

contains predominantly single domain grains with a T_C of 390 °C (Fig. 5).

Conclusions

- Nickel–zinc ferrite nano particles have been prepared by the autocatalytic decomposition of the nickel–zinc ferrous fumarato-hydrazinate at room temperature.
- The formation of ‘as synthesized’ nano-size nickel zinc ferrite was confirmed by X-ray diffraction as well as infrared spectral analysis.
- The average particle size of ‘as synthesized’ nickel zinc ferrite was found to be 20 nm.
- Saturation magnetization of ‘as synthesized’ nickel zinc ferrite was found to be 49.6 emu/g.
- The Curie temperature of ‘as synthesized’ $\text{Ni}_{0.6}\text{Zn}_{0.4}\text{Fe}_2\text{O}_4$ measured using AC susceptibility technique is found to be 390 °C.
- This work confirms that nano-size nickel zinc ferrite which finds applications in magnetic coating and

ferrofluid technology can be prepared by combustion synthesis using fumarato-hydrazinate precursor at comparatively lower temperature.

References

- Komarneni S, Fregeau E, Breval E, Roy R. Hydrothermal preparation of ultrafine ferrites and their sintering. *J Am Ceram Soc*. 1988;71(1C):26–8.
- Shrotri JJ, Kulkarni SD, Deshpande CE, Date SK. Low temperature synthesis of Ni–Zn ferrite powder and its characterization. *Mater Lett*. 1996;27:293–6.
- Jadhav SS, Shirasath SE, Toksha BG, Shukla SJ, Jadhav KM. Effect of cation proportion on the structural and magnetic properties of Ni–Zn Ferrites nano-size particles prepared by co-precipitation technique. *Chin J Chem Phys*. 2008;21(4):381–6.
- Bueno AR, Gregori ML, Nobrega MCS. Effect of Mn substitution on the microstructure and magnetic properties of $\text{Ni}_{0.50-x}\text{Zn}_{0.50-x}\text{Mn}_x\text{Fe}_2\text{O}_4$ ferrite prepared by the citrate-nitrate precursor method. *Mater Chem Phys*. 2007;105:229–33.
- Tartaj P, Morales MDP, Veintemillas-Verdaguer S, González-Carreño T, Serna CJ. The preparation of magnetic nanoparticles for applications in biomedicine. *J Phys D*. 2003;36R:182–97.
- Hankare PP, Kamle PD, Kadam MR, Rane KS, Vasambekar PN. Effect of sintering temperature on the properties of Cu–Co ferrites prepared by oxalate precipitation method. *Mater Lett*. 2007;61:2769–71.
- Randhwara BS, Kaur M, Gandotra K. Mössbauer studies on the thermolysis of manganese tris(malonato)ferrate(III)hexahydrate. *J Radioanal Nucl Chem*. 2006;269(3):69–74.
- Parvatheeewara Rao B, Mahesh Kumar A, Rao KH, Murthy YLN, Caltun OF, Dumitru I, Spinu L. Synthesis and magnetic studies of Ni–Zn ferrite nanoparticles. *J Optoelectron Adv Mater*. 2006;8(5):1703–5.
- Verma A, Goel TC, Mendiratta RG, Kishan P. Magnetic properties of nickel–zinc ferrites prepared by the citrate precursor method. *J Magn Magn Mater*. 2000;208(1):13–9.
- Zahi S, Hashim M, Daud AR. Synthesis, magnetic properties and microstructure of Ni–Zn ferrite by sol–gel technique. *J Magn Magn Mater*. 2007;308(2):177–82.
- Costa ACFM, Tortella E, Morelli MR, Kiminami RHGA. Synthesis, microstructure and magnetic properties of Ni–Zn ferrites. *J Magn Magn Mater*. 2003;256(1–3):174–82.
- Kikukawa N, Takemori M, Nagano Y, Sagasawa M, Kobayashi S. Synthesis and magnetic properties of nanostructured spinel ferrites using a glycine–nitrate process. *J Magn Magn Mater*. 2004;284:206–14.
- Priyadharsini P, Pradeep A, Chandrasekaran G. Novel combustion route of synthesis and characterization of nanocrystalline mixed ferrites of Ni–Zn. *J Magn Magn Mater*. 2009;321(12):03–1898.
- Mangalaraja RV, Ananthakumar S, Manohar P, Gnanam FD, Awano M. Microwave-flash combustion synthesis of $\text{Ni}_{0.8}\text{Zn}_{0.2}\text{Fe}_2\text{O}_4$ and its dielectric characterization. *Mater Lett*. 2004;58(10):1593–6.
- Carp O, Patron L, Pascu G, Mindru L, Stanica N. Thermal investigations of nickel–zinc ferrites formation from malate coordination compounds. *J Therm Anal Calorim*. 2006;84(2):391–4.
- Gajapathy D, Patil KC, Pai Vernekar VR. Low temperature ferrite formation using metal oxalate hydrazinate precursor. *Mater Res Bull*. 1982;17(1):29–32.
- Randhwara BS, Kaur S, Bassi PS. Thermal decomposition of strontium and barium malonates. *J Therm Anal Calorim*. 1999;55(3):789–96.

18. Mahesh GV, Patil KC. Thermal reactivity of metal acetate hydrazinates. *Thermochim Acta*. 1986;99(1):153–8.
19. Randhawa BS, Dosanjh HS, Kumar N. Synthesis of potassium ferrite by precursor and combustion methods a comparative study. *J Therm Anal Calorim*. 1999;95(1):75–80.
20. Sivasankar BN. Cobalt(II), nickel(II) and zinc(II) dicarboxylate complexes with hydrazine as bridged ligand characterization and thermal degradation. *J Therm Anal Calorim*. 2006;86(2):385–92.
21. Sivasankar BN, Govindarajan S. Studies on bis(hydrazine) metal malonates and succinates. *Synth React Inorg Met-Org Chem*. 1994;24(9):1573–82.
22. Sivasankar BN, Govindarajan S. Hydrazine mixed metal malonates—new precursors for metal cobaltites. *Mater Res Bull*. 1996;31(1):47–54.
23. Verenkar VMS, Porob RA, Sawant SY, Kannan KR. Synthesis, characterisation and thermal analysis of nickel manganese succinato-hydrazinate. In: Singh Mudher KD, Bharadwaj S, Ravindran PV, Sali SK, Venugopal V, editors. Proceedings of the 14th national symposium on thermal analysis, Thermans. Vadodara: Indian Thermal Analysis Society; 2004. p. 335–7.
24. Sivasankar BN, Govindarajan S. Acetate and malonate complexes of cobalt(II), nickel(II) and zinc(II) with hydrazinium cation: preparation, spectral and thermal studies. *J Therm Anal*. 1997; 48(6):1401–13.
25. Rane KS, Verenkar VMS. Synthesis of ferrite grade γ - Fe_2O_3 . *Bull Mater Sci*. 2001;24(1):39–45.
26. Randhawa BS, Kaur M. A comparative study on the thermal decomposition of some transition metal maleates and fumarates. *J Therm Anal Calorim*. 2007;89(1):251–5.
27. Khalil I, Petit-Ramel MM. Polynuclear complexes quantitative and qualitative study of copper-yttrium malate and copper-uranyl malate. *J Inorg Nucl Chem*. 1979;41(5):711–6.
28. Gawas UB, Mojumdar SC, Verenkar VMS. $\text{Ni}_{0.5}\text{Mn}_{0.1}\text{Zn}_{0.4}\text{Fe}_2(\text{C}_4\text{H}_2\text{O}_4)_3\cdot6\text{N}_2\text{H}_4$ precursor $\text{Ni}_{0.5}\text{Mn}_{0.1}\text{Zn}_{0.4}\text{Fe}_2\text{O}_4$ nanoparticles preparation, IR spectral, XRD, SEM-EDS and thermal analysis. *J Therm Anal Calorim*. 2009;96(1):49–52.
29. Gonsalves LR, Verenkar VMS, Mojumdar SC. Preparation and characterization of $\text{Co}_{0.5}\text{Zn}_{0.5}\text{Fe}_2(\text{C}_4\text{H}_2\text{O}_4)_3\cdot6\text{N}_2\text{H}_4$: a precursor to prepare $\text{Co}_{0.5}\text{Zn}_{0.5}\text{Fe}_2\text{O}_4$ nanoparticles. *J Therm Anal Calorim*. 2009;96(1):53–7.
30. More A, Verenkar VMS, Mojumdar SC. Nickel ferrite nanoparticles synthesis from novel fumarato-hydrazinate precursor. *J Therm Anal Calorim*. 2008;94(1):63–7.
31. Sawant SY, Verenkar VMS, Mojumdar SC. Preparation, thermal, XRD, chemical and FTIR spectral analysis of NiMn_2O_4 nanoparticles and respective precursor. *J Therm Anal Calorim*. 2007; 90(3):669–72.
32. Porob RA, Khan SZ, Mojumdar SC, Verenkar VMS. Synthesis, TG, DSC and infrared spectral study of $\text{NiMn}_2(\text{C}_4\text{H}_4\text{O}_4)_3\cdot6\text{N}_2\text{H}_4$: a precursor for NiMn_2O_4 nanoparticles. *J Therm Anal Calorim*. 2006;86(3):605–8.
33. Gawas U, Bhattacharya S, More A, Verenkar VMS. Synthesis and characterization of $\text{Ni}_{0.6}\text{Zn}_{0.4}\text{Fe}_2\text{O}_4$ obtained by self-propagating auto-combustion of a novel precursor. In: Lokhande CD, editor. Proceedings of the international conference on advanced materials and applications. Kolhapur, India; 2007. p. 86–93.
34. Gawas UB, Verenkar VMS. Synthesis, characterizations, thermal and infrared spectral studies of manganese nickel zinc ferrous fumarato-hydrazinate complex. In: Kalsi PC, Pai RV, Pai MR, Bharadwaj SR, Venugopal V, editors. Proceedings of the 17th national symposium on thermal analysis, Thermans. Haryana: Indian Thermal Analysis Society; 2010. p. 174–6.
35. Vogel's, Text book of quantitative inorganic analysis (revised by Jeffery GH, Bassett, Mendham J and Denney RC), 5th edn. London: Longman; 1989. p. 402.
36. Likhite SD, Radhakrishnamurthy C, Sahasrabudhe PW. Alternating current electromagnet type hysteresis loop tracer for minerals and rocks. *Rev Sci Instrum*. 1965;36(11):1558–60.
37. Likhite SD, Radhakrishnamurthy C. Initial susceptibility and constricted Rayleigh loops of some basalts. *Curr Sci*. 1966;35: 534–6.
38. Braibanti A, Dallavalle F, Pellinghelli MA, Leporati E. The nitrogen–nitrogen stretching band in hydrazine derivatives and complexes. *Inorg. Chem*. 1968;7:1430–3.
39. Tsuchiya R, Yonemura M, Uehara A, Kyuno E. Derivatographic studies on transition metal complexes. XIII. Thermal decomposition of $[\text{Ni}(\text{N}_2\text{H}_4)_6]\text{X}_2$ complexes. *Bull Chem Soc Jpn*. 1974;47(3):660–4.
40. Nakamoto K. Infrared and Raman spectra of inorganic and coordination compounds part B. 6th ed. New York: John Wiley; 1978. p. 13.
41. Waldron RD. Infrared spectra of ferrites. *Phys Rev*. 1955;99: 1727–35.
42. Akther Hossain AKM, Mahmud ST, Seki M, Kawai T, Tabata H. Structural, electrical transport, and magnetic properties of $\text{Ni}_{1-x}\text{Zn}_x\text{Fe}_2\text{O}_4$. *J Magn Magn Mater*. 2007;312(1):210–9.
43. Mangalaraja RV, Ananthakumar S, Manohar P, Gnanam FD, Awano M. Direct current resistivity studies of $\text{Ni}_{1-x}\text{Zn}_x\text{Fe}_2\text{O}_4$ prepared through flash combustion and citrate-gel decomposition techniques. *Mater Lett*. 2003;57(18):2662–5.
44. Coey JMD, Khalafalla D. Superparamagnetic γ - Fe_2O_3 . *Phys Stat Sol (A)*. 1972;11(1):229–41.